Deep impurity levels in semiconductor superlattices

Shang Yuan Ren
Department of Physics, University of Notre Dame, Notre Dame, Indiana 46556
*and Department of Physics, University of Science and Technology of China, Hefei, China**

John D. Dow and Jun Shen
Department of Physics, University of Notre Dame, Notre Dame, Indiana 46556
(Received 29 February 1988; revised manuscript received 20 October 1988)

A theory of sp^3-bonded substitutional deep impurity levels in periodic $N_1 \times N_2$ GaAs/$Al_xGa_{1-x}As$ superlattices predicts that as the thickness t(GaAs) of each GaAs layer is reduced below a critical value ($\lesssim 17$ Å or $N_1 \lesssim 6$ for $x = 0.7$) common shallow donor impurities such as Si cease donating electrons to the conduction band and instead become deep traps. This happens because the deep levels associated with point defects in either GaAs or $Al_xGa_{1-x}As$ layers (when measured relative to the valence-band maximum of GaAs) are much less sensitive to changes of the alloy composition or layer thicknesses of the superlattice than the superlattice band edges, particularly the conduction-band edge. For some compositions x, dopants such as Si are shallow donors in $N \times N$ GaAs/$Al_xGa_{1-x}As$ superlattices but deep traps in $Al_{(x/2)}Ga_{1-(x/2)}As$ alloy (the alloy obtained by disordering the superlattice). The band gap and band edges of the superlattice, and hence the ionization energies of deep levels, depend strongly on the layer thickness t(GaAs) but only weakly on $t(Al_xGa_{1-x}As)$. The T_2- and A_1-derived deep levels (of the bulk point group T_d) are split and shifted, respectively, near a GaAs/$Al_xGa_{1-x}As$ interface: the p-like T_2 level splits into an a_1 (p_z-like) level, a b_1 [(p_x+p_y)-like] level, and a b_2 [(p_x-p_y)-like] level of the point group for any general superlattice site (C_{2v}), whereas the s-like A_1 bulk level becomes an a_1 (s-like) level of C_{2v}. The order of magnitude of the shifts and splittings of deep levels at a GaAs/$Al_xGa_{1-x}As$ interface is 0.1 eV, depends on x, and becomes very small for impurities more than about three atomic planes away from an interface. Deep levels in the GaAs quantum wells experience level shifts due to (i) penetration of their wave functions into the more electropositive $Al_xGa_{1-x}As$ layers, (ii) the band offset, and (iii) quantum confinement. The cation vacancy, when brought close to a GaAs/$Al_xGa_{1-x}As$ interface, may undergo a shallow-deep transition. These predictions are based on a periodic superslab calculation for unit superslabs with total thickness t(GaAs)$+t(Al_xGa_{1-x}As)$ as large as 102 Å or $N_1+N_2=36$ two-atom-thick layers. The Hamiltonian is a tight-binding model in a hybrid basis that is a generalization of the Vogl model and properly accounts for the nature of interfacial bonds. The deep levels are computed by using the theory of Hjalmarson *et al.* and the special-points method. Our results indicate that some normally shallow donors, such as Si, can become deep levels at certain sites in the superlattice as a result of local fluctuations in alloy composition x or layer thickness t(GaAs).

I. INTRODUCTION

Modulation doping of GaAs/$Al_xGa_{1-x}As$ superlattices,[1,2] by which Si impurities are inserted into the large-band-gap $Al_xGa_{1-x}As$ layers of a superlattice but donate their electrons to the small-band-gap GaAs layers, has already played a role in the development of high-speed III-V-compound semiconductive devices. However, practical devices based on $Al_xGa_{1-x}As$ often are limited to alloy compositions $x < 0.3$ because of the inability of Si to dope n type for $x > 0.3$,[3] apparently because of the formation of Si-related centers that are deep traps.[3-11] Furthermore, some devices, such as HEMT's (high-electron-mobility transistors) operate using quantum-well structures[12] at or near GaAs/$Al_xGa_{1-x}As$ interfaces, and the performance of these devices depends on the doping (e.g., by Si), the alloy composition x, and the superlattice structure.[13] Clearly, a theory of impurity levels in superlattices and heterostructures is needed to understand the conditions under which a specific impurity produces shallow donor levels and "dopes" the semiconductor versus the conditions for deep-trap formation and the trapping of carriers. That is the purpose of this paper. Das Sarma and Madhukar[14] have previously discussed the deep levels of vacancies in some superlattices, but, to our knowledge, the present work is one of the first systematic studies of the chemical trends of deep impurity levels in superlattices.[15,16] We do know that Hjalmarson,[17] Nelson *et al.*,[18] and Lannoo and Bourgoin[19] are studying deep levels in parallel with our effort, however, although we are not fully aware of the current state of their work. This is also the first treatment of defects in large-layer superlattices: we consider unit supercells typically 40 atomic planes thick. The theory developed here is an extension to superlattices of the theory of Hjalmarson *et al.*[20] of deep impurity levels

in the bulk, which has successfully predicted deep levels and their wave functions.[21–23]

II. FORMALISM

A. Host Hamiltonian

We treat a periodic GaAs/$Al_xGa_{1-x}As$ superlattice whose layers are perpendicular to the [001] direction. We employ a nearest-neighbor tight-binding Hamiltonian with an s^*sp^3 basis of five orbitals at each site. Our Hamiltonian, in the limit $x=0$, is identical to the Vogl model for GaAs. Some differences are introduced because of the superlattice, which we treat using a superhelix or supercell method. The superlattice we consider has N_1 two-atom-thick layers of GaAs and N_2 two-atom-thick layers of $Al_xGa_{1-x}As$ repeated periodically; the GaAs and $Al_xGa_{1-x}As$ are assumed to be perfectly lattice matched. We denote this superlattice either as a $(GaAs)_{N_1}/(Al_xGa_{1-x}As)_{N_2}$ superlattice, or as a GaAs/$Al_xGa_{1-x}As$ superlattice with N_1 GaAs layers and N_2 $Al_xGa_{1-x}As$ layers, or as an $N_1\times N_2$ GaAs/$Al_xGa_{1-x}As$ superlattice.

We first define (for the case $x=1$) a *superhelix* or supercell as a helical string with axis aligned along the [001] or z direction consisting of $2N_1+2N_2$ adjacently bonded atoms As, Ga, As, Ga, As, . . . , Ga, As, Al, As, Al, As, Al, . . . , As, Al. (For $x\neq 1$, replace Al, by Al_xGa_{1-x}.) The center of this helix is at $\mathbf{L}$ and each of the atoms of the helix is at position $\mathbf{L}+\mathbf{v}_\beta$ (for $\beta=0,1,2,\ldots,2N_1+2N_2-1$). A *superslab* of GaAs/$Al_xGa_{1-x}As$ consists of all such helices with the same value of L_z and all possible different values of L_x and L_y, and the superlattice is a stacked array of these superslabs. If the origin of coordinates is taken to be at an As atom, the x and y axes are oriented such that a neighboring cation is at $(\frac{1}{4},\frac{1}{4},\frac{1}{4})a_L$, where a_L is the lattice constant. At each site there are s^*sp^3 basis orbitals $|n,\mathbf{L},\mathbf{v}_\beta)$, where $n=s^*$, s, p_x, p_y, or p_z, and $\beta=0,1,2,\ldots,2N_1+2N_2-1$. From these basis orbitals we form the sp^3 hybrid orbitals at each site $\mathbf{R}=(\mathbf{L},\mathbf{v}_\beta)$.

The hybrid orbitals are

$$
\begin{aligned}
|h_1,\mathbf{R}\rangle&=[\,|s,\mathbf{R}\rangle+\lambda|p_x,\mathbf{R}\rangle+\lambda|p_y,\mathbf{R}\rangle+\lambda|p_z,\mathbf{R}\rangle]/2\ ,\\
|h_2,\mathbf{R}\rangle&=[\,|s,\mathbf{R}\rangle+\lambda|p_x,\mathbf{R}\rangle-\lambda|p_y,\mathbf{R}\rangle-\lambda|p_z,\mathbf{R}\rangle]/2\ ,\\
|h_3,\mathbf{R}\rangle&=[\,|s,\mathbf{R}\rangle-\lambda|p_x,\mathbf{R}\rangle+\lambda|p_y,\mathbf{R}\rangle-\lambda|p_z,\mathbf{R}\rangle]/2\ ,
\end{aligned}
$$

and

$$
|h_4,\mathbf{R}\rangle=[\,|s,\mathbf{R}\rangle-\lambda|p_x,\mathbf{R}\rangle-\lambda|p_y,\mathbf{R}\rangle+\lambda|p_z,\mathbf{R}\rangle]/2\ , \tag{1}
$$

where $\lambda=+1$ (-1) for atoms at anion (cation) sites. Next, we introduce the label $\nu=s^*$, h_1, h_2, h_3, or h_4, and our hybrid basis orbitals are $|\nu,\mathbf{R}\rangle$. In terms of these orbitals we form the tight-binding orbitals[24]

$$
|\nu,\beta,\mathbf{k}\rangle=N_s^{-1/2}\sum_{\mathbf{L}}\exp(i\mathbf{k}\cdot\mathbf{L}+i\mathbf{k}\cdot\mathbf{v}_\beta)\,|\nu,\mathbf{L},\mathbf{v}_\beta\rangle\ , \tag{2}
$$

where $\mathbf{k}$ is (in a reduced-zone scheme) any wave vector of the minizone or (in an extended-zone scheme) any wave vector of the zinc-blende Brillouin zone. Here, N_s is the number of supercells.

The minizone wave vector is a good quantum number, and so the tight-binding Hamiltonian is diagonal in $\mathbf{k}$. Evaluation of the matrix elements $(\nu,\beta,\mathbf{k}\,|\,H\,|\,\nu',\beta',\mathbf{k})$ leads to a tight-binding Hamiltonian of the block-tridiagonal form. For different β and β', the first three rows of block matrices are

$$
\begin{pmatrix}
H(0,0) & H(0,1) & 0 & \cdots & \cdots & \cdots & 0 & H(0,2N_1+2N_2-1)\\
H^*(0,1) & H(1,1) & H(1,2) & 0 & 0 & \cdots & 0 & 0\\
0 & H^*(1,2) & H(2,2) & H(2,3) & 0 & \cdots & 0 & 0\\
\vdots & \vdots & \vdots & & & & & \vdots
\end{pmatrix}. \tag{3}
$$

The last row of blocks is

$$
\begin{pmatrix}
\vdots & & \vdots & \vdots & & & & \vdots\\
H^*(0,2N_1+2N_2-1) & 0 & 0 & \cdots & 0 & H^*(2N_1+2N_2-2,2N_1+2N_2-1) & H(2N_1+2N_2-1,2N_1+2N_2-1)
\end{pmatrix}. \tag{4}
$$

Here, $H(\beta,\beta')$ depends on $\mathbf{k}$ and is given in terms of various 5×5 matrices for different ν and ν'.

The diagonal (in β) 5×5 matrix, $H(\beta,\beta)$ at site β, is

$$
H(\beta,\beta)=(\nu,\beta,\mathbf{k}\,|\,H\,|\,\nu',\beta,\mathbf{k})=\begin{pmatrix}
\varepsilon_{s^*} & 0 & 0 & 0 & 0\\
0 & \varepsilon_h & T & T & T\\
0 & T & \varepsilon_h & T & T\\
0 & T & T & \varepsilon_h & T\\
0 & T & T & T & \varepsilon_h
\end{pmatrix}, \tag{5}
$$

where

$$
\varepsilon_h=(\varepsilon_s+3\varepsilon_p)/4 \tag{6}
$$

is the hybrid energy, and

$$
T=(\varepsilon_s-\varepsilon_p)/4 \tag{7}
$$

is the hybrid-hybrid interaction; the energies ε_{s^*}, ε_h, and T in $H(\beta,\beta)$ refer to the atom at the βth site, and may be obtained from the energies w tabulated by Vogl *et al.*[25] To account for the observed[26] valence-band-edge discon-

tinuity of 32% of the direct band gap,[27] a constant is added to ε_{s^*} and ε_h for $Al_xGa_{1-x}As$; this constant is adjusted to give the valence-band maximum of $Al_xGa_{1-x}As$ below the valence-band maximum of GaAs by 32% of the direct-band-gap difference in the limit $N_1=N_2\to\infty$.

The off-diagonal matrix elements $(\nu,\beta,\mathbf{k}\mid H\mid\nu',\beta',\mathbf{k})$ or $H(\beta,\beta')$ are best expressed in terms of matrix elements of H between s^*, s, and p orbitals. This is accomplished by the transformation

$$(\nu,\beta,\mathbf{k}\mid H\mid\nu',\beta',\mathbf{k})=\sum_{n,n'}C(\nu,n;\beta)C(\nu',n';\beta')(n,\beta,\mathbf{k}\mid H\mid n',\beta',\mathbf{k})\ , \tag{8}$$

where we have the s^*sp^3 tight-binding functions

$$\mid n,\beta,\mathbf{k})=N_s^{-1/2}\sum_{\mathbf{L}}\exp(i\mathbf{k}\cdot\mathbf{L}+i\mathbf{k}\cdot\mathbf{v}_\beta)\mid n,\mathbf{L},\mathbf{v}_\beta)\ , \tag{9}$$

and the 5×5 matrices $C(\nu,n;\beta)$ are

$$C(\nu,n;\beta)=\begin{array}{c}\\ s^*\\ h_1\\ h_2\\ h_3\\ h_4\end{array}\begin{array}{c}\begin{array}{ccccc}s^* & s & p_x & p_y & p_z\end{array}\\ \begin{pmatrix}1&0&0&0&0\\0&\frac{1}{2}&+\lambda/2&+\lambda/2&+\lambda/2\\0&\frac{1}{2}&+\lambda/2&-\lambda/2&-\lambda/2\\0&\frac{1}{2}&-\lambda/2&+\lambda/2&-\lambda/2\\0&\frac{1}{2}&-\lambda/2&-\lambda/2&+\lambda/2\end{pmatrix}\end{array}\ , \tag{10}$$

where $\lambda=+1\ (-1)$ if β refers to an anion (cation).

There are several distinct cases for which the off-diagonal (in β) matrix elements $(n,\beta,\mathbf{k}\mid H\mid n',\beta',\mathbf{k})$ are nonzero (for $\beta\neq\beta'$).

1. *Intramaterial matrix elements*

If β and β' both refer to nearest-neighbor sites in the same material (either the GaAs or the $Al_xGa_{1-x}As$), we have (assuming β and β' are in material number 1, the GaAs), for example,

$$(n,\beta,\mathbf{k}\mid H\mid n',\beta',\mathbf{k})=H_{c1a1}\ , \tag{11}$$

if β refers to a cation and β' refers to an anion. H_{c1a1} is a 5×5 matrix whose rows and columns are labeled by n, which ranges over the values s^*, s, p_x, p_y, and p_z. Similarly, we have matrix elements H_{a1c1}, H_{a2c2}, and H_{c2a2}. These matrix elements are

$$H_{c1a1}=\begin{pmatrix}0&0&-V(s^*c,pa)g^*_{1ca}&-V(s^*c,pa)g^*_{1ca}&-V(s^*c,pa)g^*_{0ca}\\0&V(s,s)g^*_{0ca}&-V(sc,pa)g^*_{1ca}&-V(sc,pa)g^*_{1ca}&-V(sc,pa)g^*_{0ca}\\V(s^*a,pc)g^*_{1ca}&V(sa,pc)g^*_{1ca}&V(x,x)g^*_{0ca}&V(x,y)g^*_{0ca}&V(x,y)g^*_{1ca}\\V(s^*a,pc)g^*_{1ca}&V(sa,pc)g^*_{1ca}&V(x,y)g^*_{0ca}&V(x,x)g^*_{0ca}&V(x,y)g^*_{1ca}\\V(s^*a,pc)g^*_{0ca}&V(sa,pc)g^*_{0ca}&V(x,y)g^*_{1ca}&V(x,y)g^*_{1ca}&V(x,x)g^*_{0ca}\end{pmatrix} \tag{12}$$

and

$$H_{a1c1}=\begin{pmatrix}0&0&V(s^*a,pc)g_{1ac}&-V(s^*a,pc)g_{1ac}&-V(s^*a,pc)g_{0ac}\\0&V(s,s)g_{0ac}&V(sa,pc)g_{1ac}&-V(sa,pc)g_{1ac}&-V(sa,pc)g_{0ac}\\-V(s^*c,pa)g_{1ac}&-V(sc,pa)g_{1ac}&V(x,x)g_{0ac}&-V(x,y)g_{0ac}&-V(x,y)g_{1ac}\\V(s^*c,pa)g_{1ac}&V(sc,pa)g_{1ac}&-V(x,y)g_{0ac}&V(x,x)g_{0ac}&V(x,y)g_{1ac}\\V(s^*c,pa)g_{0ac}&V(sc,pa)g^*_{0ac}&-V(x,y)g^*_{1ac}&V(x,y)g_{1ac}&V(x,x)g_{0ac}\end{pmatrix}\ . \tag{13}$$

All of the matrix elements V are those tabulated by Vogl *et al.*[25] for material number 1 (viz., GaAs). Identical expressions exist for H_{a2c2} and H_{c2a2}, with $Al_xGa_{1-x}As$ matrix elements. (The $Al_xGa_{1-x}As$ matrix elements are obtained by a virtual-crystal average of the Vogl matrix elements for AlAs and GaAs: x times the corresponding AlAs matrix elements plus $1-x$ times the GaAs matrix elements.)

2. Intermaterial matrix elements

At the interface between GaAs and $Al_xGa_{1-x}As$ there will be nonzero matrix elements of H for each bond between nearest neighbors. These are H_{a2c1} and H_{c2a1}:

$$H_{a2c1}=\begin{bmatrix} 0 & 0 & V(s^*a,pc)g_{1ac} & -V(s^*a,pc)g_{1ac} & -V(s^*a,pc)g_{0ac} \\ 0 & V(s,s)g_{0ac} & V(sa,pc)g_{1ac} & -V(sa,pc)g_{1ac} & -V(sa,pc)g_{0ac} \\ -V(s^*c,pa)g_{1ac} & -V(sc,pa)g_{1ac} & V(x,x)g_{0ac} & -V(x,y)g_{0ac} & -V(x,y)g_{1ac} \\ V(s^*c,pa)g_{1ac} & V(sc,pa)g_{1ac} & -V(x,y)g_{0ac} & V(x,x)g_{0ac} & V(x,y)g_{1ac} \\ V(s^*c,pa)g_{0ac} & V(sc,pa)g_{0ac} & -V(x,y)g_{1ac} & V(x,y)g_{1ac} & V(x,x)g_{0ac} \end{bmatrix} \tag{14}$$

and

$$H_{c2a1}=\begin{bmatrix} 0 & 0 & -V(s^*c,pa)g^*_{1ac} & V(s^*c,pa)g^*_{1ac} & V(s^*c,pa)g^*_{0ac} \\ 0 & V(s,s)g^*_{0ac} & -V(sc,pa)g^*_{1ac} & V(sc,pa)g^*_{1ac} & V(sc,pa)g^*_{0ac} \\ V(s^*a,pc)g^*_{1ac} & V(sa,pc)g^*_{1ac} & V(x,x)g^*_{0ac} & -V(x,y)g^*_{0ac} & -V(x,y)g^*_{1ac} \\ -V(s^*a,pc)g^*_{1ac} & -V(sa,pc)g^*_{1ac} & -V(x,y)g^*_{0ac} & V(x,x)g^*_{0ac} & V(x,y)g^*_{1ac} \\ -V(s^*a,pc)g^*_{0ac} & -V(sa,pc)g^*_{0ac} & -V(x,y)g^*_{1ac} & V(x,y)g^*_{1ac} & V(x,x)g^*_{0ac} \end{bmatrix} . \tag{15}$$

Here the Vogl matrix elements are those for the bond in question: If the cation is Al_xGa_{1-x} and the anion is As, then the matrix element is the $Al_xGa_{1-x}As$ matrix element obtained by a virtual-crystal average of the AlAs and GaAs values. We also have

$$g_{0ca}=\exp(i\mathbf{k}\cdot\mathbf{d}_1)+\exp(i\mathbf{k}\cdot\mathbf{d}_4) ,$$

$$g_{1ca}=\exp(i\mathbf{k}\cdot\mathbf{d}_1)-\exp(i\mathbf{k}\cdot\mathbf{d}_4) ,$$

$$g_{0ac}=\exp(i\mathbf{k}\cdot\mathbf{d}_2)+\exp(i\mathbf{k}\cdot\mathbf{d}_3) ,$$

and

$$g_{1ac}=\exp(i\mathbf{k}\cdot\mathbf{d}_2)-\exp(i\mathbf{k}\cdot\mathbf{d}_3) , \tag{16}$$

where we have $4\mathbf{d}_i/a_L=(1,1,1)$, $(1,-1,-1)$, and $(-1,1,-1)$, and $(-1,-1,1)$ for $i=1$, 2, 3, and 4, respectively. Here, a_L is the room-temperature lattice constant of GaAs, 5.653 Å, which we assume is equal to that of $Al_xGa_{1-x}As$.[28]

In this work we study deep impurity levels in superhelices as large as $N_1+N_2=20$; that is, in 40-atom-thick superslabs.[29] The dimension of the Hamiltonian matrix at each value of $\mathbf{k}$ is $5(2N_1+2N_2)$, because there are five orbitals per site. We diagonalize this Hamiltonian numerically for each (special point) $\mathbf{k}$, finding its eigenvalues $E_{\gamma,\mathbf{k}}$ and the projections of the eigenvectors $|\gamma,\mathbf{k}\rangle$ on the $|\nu,\beta,\mathbf{k}\rangle$ hybrid basis: $(\nu,\beta,\mathbf{k}|\gamma,\mathbf{k}\rangle$. Here, γ is the band index (and ranges from 1 to 200 for $N_1=N_2=10$) and $\mathbf{k}$ lies within the mini-Brillouin zone in a reduced-zone scheme or within the GaAs Brillouin zone in an extended-zone scheme. (We assume that GaAs and $Al_xGa_{1-x}As$ are perfectly lattice-matched.[28])

B. Deep levels

The theory of deep levels is based on the Green's-function theory of Hjalmarson *et al.*,[20] which solves the secular equation for the deep-level energy E,

$$\det[1-G(E)V] =0=\det\left[1-\mathrm{P}\int\left[\delta(E'-H)\frac{V}{E-E'}\right]dE'\right] . \tag{17}$$

Here, V is the defect potential matrix,[20] which is zero except at the defect site and diagonal on that site, $(0,V_s,V_p,V_p,V_p)$, in the Vogl s^*sp^3 local basis centered on each atom. We also have $G=(E-H)^{-1}$, where H is the host tight-binding Hamiltonian operator. The spectral density operator is $\delta(E'-H)$ and P denotes the principal-value integral over all energies. In the fundamental band gap of the superlattice, G is real.

1. Point-group analysis

A substitutional point defect in either bulk GaAs or bulk $Al_xGa_{1-x}As$ has tetrahedral (T_d) point-group symmetry (assuming a virtual-crystal approximation for $Al_xGa_{1-x}As$). Each such sp^3-bonded defect normally has one s-like (A_1) and one triply-degenerate p-like (T_2) deep defect level near the fundamental band gap. If we imagine breaking the symmetry of bulk GaAs by making it into a GaAs/GaAs superlattice along the [001] direction, we reduce the T_d symmetry to D_{2d}. If, in addition, we change alternating slabs of GaAs to virtual-crystal $Al_xGa_{1-x}As$, forming a GaAs/$Al_xGa_{1-x}As$ superlattice, then the point-group symmetry of a general substitutional defect is C_{2v}. (For selected sites, e.g., at the center of a material, the symmetry can be higher.) Note that the C_{2v} symmetry we find differs from that of Ref. 14. In the GaAs/$Al_xGa_{1-x}As$ superlattice the A_1 and T_2 deep levels of the bulk GaAs or $Al_xGa_{1-x}As$ produce two a_1 levels (one s-like, derived from the A_1 level, and one T_2-derived p_z-like), one b_1 level [(p_x+p_y)-like], and one b_2

level [(p_x-p_y)-like]. Of course, for impurities far from a GaAs/Al_xGa_{1-x}As interface, the s-like a_1 level will have an energy very close to the energy of a bulk A_1 level, and the p_z-like a_1 level and the b_1 and b_2 levels will lie close to the bulk T_2 level also. We normally expect to find the T_2-derived a_1 level between the b_1 and b_2 levels, but if the level lies close to the valence-band maximum, then the splitting of the valence-band edge into a (p_x+p_y)- and (p_x-p_y)-like maximum with a p_z-like edge at slightly lower energy (because of the smaller effective mass) may cause the a_1 deep level to lie lower in energy than the b_1 and b_2 levels by a comparable energy [see Eq. (17)]. Note that this splitting exists even for defects distant from the interface and is a consequence of the different host spectral densities in the superlattice for a_1 and b_1 and b_2 states.

2. Secular equations

The secular equation, Eq. (17), is reduced by symmetry to the following three equations:

$$G(b_1;E)=V_p^{-1} \text{ for } b_1 \text{ levels} , \tag{18}$$

$$G(b_2;E)=V_p^{-1} \text{ for } b_2 \text{ levels} , \tag{19}$$

and

$$\det\begin{bmatrix} G(s,s;E)V_s-1 & G(s,z;E)V_p \\ G(z,s;E)V_s & G(z,z;E)V_p-1 \end{bmatrix}=0 , \tag{20}$$

for a_1 levels, where we have

$$G(b_1;E)=\sum_{\gamma,\mathbf{k}} \frac{|\langle h_1,\beta,\mathbf{k}\,|\,\gamma,\mathbf{k}\rangle-\langle h_4,\beta,\mathbf{k}\,|\,\gamma,\mathbf{k}\rangle|^2}{2(E-E_{\gamma,\mathbf{k}})} , \tag{21}$$

$$G(b_2;E)=\sum_{\gamma,\mathbf{k}} \frac{|\langle h_2,\beta,\mathbf{k}\,|\,\gamma,\mathbf{k}\rangle-\langle h_3,\beta,\mathbf{k}\,|\,\gamma,\mathbf{k}\rangle|^2}{2(E-E_{\gamma,\mathbf{k}})} , \tag{22}$$

$$G(s,s;E)=\sum_{\gamma,\mathbf{k}} \frac{|\langle h_1,\beta,\mathbf{k}\,|\,\gamma,\mathbf{k}\rangle+\langle h_2,\beta,\mathbf{k}\,|\,\gamma,\mathbf{k}\rangle+\langle h_3,\beta,\mathbf{k}\,|\,\gamma,\mathbf{k}\rangle+\langle h_4,\beta,\mathbf{k}\,|\,\gamma,\mathbf{k}\rangle|^2}{4(E-E_{\gamma,\mathbf{k}})} , \tag{23}$$

$$G(z,z;E)=\sum_{\gamma,\mathbf{k}} \frac{|\langle h_1,\beta,\mathbf{k}\,|\,\gamma,\mathbf{k}\rangle-\langle h_2,\beta,\mathbf{k}\,|\,\gamma,\mathbf{k}\rangle-\langle h_3,\beta,\mathbf{k}\,|\,\gamma,\mathbf{k}\rangle+\langle h_4,\beta,\mathbf{k}\,|\,\gamma,\mathbf{k}\rangle|^2}{4(E-E_{\gamma,\mathbf{k}})} , \tag{24}$$

and

$$G(s,z;E)=\sum_{\gamma,\mathbf{k}} [\langle h_1,\beta,\mathbf{k}\,|\,\gamma,\mathbf{k}\rangle+\langle h_2,\beta,\mathbf{k}\,|\,\gamma,\mathbf{k}\rangle+\langle h_3,\beta,\mathbf{k}\,|\,\gamma,\mathbf{k}\rangle+\langle h_4,\beta,\mathbf{k}\,|\,\gamma,\mathbf{k}\rangle] \times[\langle h_1,\beta,\mathbf{k}\,|\,\gamma,\mathbf{k}\rangle-\langle h_2,\beta,\mathbf{k}\,|\,\gamma,\mathbf{k}\rangle-\langle h_3,\beta,\mathbf{k}\,|\,\gamma,\mathbf{k}\rangle+\langle h_4,\beta,\mathbf{k}\,|\,\gamma,\mathbf{k}\rangle]^*[4(E-E_{\gamma,\mathbf{k}})]^{-1} . \tag{25}$$

Here, $G(z,s;E)$ is the Hermitian conjugate of $G(s,z;E)$ and β is the site of the defect in the superlattice.

For each β the relevant host Green's functions, Eqs. (21)–(25), are evaluated using the special-points method,[30] and the secular equations (18)–(20) are solved, yielding $E(b_1;V_p)$, $E(b_2;V_p)$, and two values of $E(a_1;V_s,V_p)$. The defect-potential matrix elements V_s and V_p are obtained using a slight modification of Hjalmarson's approach.[31,32] For $N_1=N_2=10$, there are 40 possible sites β, each with four relevant deep levels: two a_1, one b_1, and one b_2; thus there are 160 levels.

3. Special points

For our studies of deep levels in the band gaps of superlattices, we consider only superlattices such that $(N_1+N_2)/4$ is an integer. In such cases the sums over $\mathbf{k}$ in Eqs. (21)–(25) can be performed using 12 special points $\mathbf{k}=(\pi/4a_L)\mathbf{u}$, where we have the value $\mathbf{u}$ and the weight w of each special point $(\mathbf{u};w)$:[30] $(7,3,1;\frac{1}{8})$, $(5,3,1;\frac{1}{16})$, $(7,1,1;\frac{1}{16})$, $(3,1,1;\frac{1}{8})$, $(3,3,1;\frac{1}{16})$, $(1,1,1;\frac{1}{16})$, $(-7,3,-1;\frac{1}{8})$, $(-5,3,-1;\frac{1}{16})$, $(-7,1,-1;\frac{1}{16})$, $(-3,1,-1;\frac{1}{8})$, $(-3,3,-1;\frac{1}{16})$, and $(-1,1,-1;\frac{1}{16})$. For $(N_1+N_2)/4$ an integer and a GaAs/GaAs superlattice, either the first six or the last six special points would be sufficient to give the Green's function at any site in the superlattice with the same accuracy as Chadi's and Cohen's[33] ten special points for bulk GaAs, which are known to give an adequately accurate bulk Green's function. However, for the GaAs/Al_xGa_{1-x}As superlattice, 12 special points are necessary because of the reduction of symmetry from D_{2d} to C_{2v} from GaAs/GaAs to GaAs/Al_xGa_{1-x}As.

III. RESULTS

A. Host band gap

Our calculations produce $E_{\gamma,\mathbf{k}}$, the superlattice band structure, including the band gap, which exhibits a particularly interesting behavior as the thickness of the GaAs slabs, $t(\text{GaAs})=N_1a_1/2$ (where $a_1=5.653$ Å is the lattice constant of GaAs), or the number of GaAs layers, N_1, becomes small in comparison with the thickness, $t(Al_xGa_{1-x}As)=N_2a_2/2$,[28] or the number of layers, N_2,

of $Al_xGa_{1-x}As$ slabs: The small-band-gap GaAs layers become quantum wells surrounded by large-band-gap $Al_xGa_{1-x}As$ (Fig. 1). As a result, the band gap of the superlattice increases from the GaAs band gap toward the $Al_xGa_{1-x}As$ band gap as N_1 decreases (for N_2 large). (Qualitatively similar results for smaller N_1+N_2 superlattices have been reported by Schulman and McGill for GaAs/AlAs superlattices.[34]) This is demonstrated by the calculated results of Figs. 2 and 3. The band gap was taken to be the smallest gap found at one of the following $\mathbf{k}=(2\pi/a_L)\mathbf{S}$ points of the mini-Brillouin-zone: $\mathbf{S}=(0,0,0)$, $(0,0,\tau)$, $(\frac{1}{2},\frac{1}{2},\tau)$, $(\frac{1}{2},\frac{1}{2},0)$, $(1,0,\tau)$, and $(1,0,0)$, where we have $\tau=(N_1+N_2)^{-1}$. For N_1 large, the gap was invariably at $\mathbf{k}=\Gamma=(0,0,0)$, but for small N_1 and large x (somewhat larger than 0.3) it was sometimes found at $\mathbf{S}=(\frac{1}{2},\frac{1}{2},\tau)$ or $(\frac{1}{2},\frac{1}{2},0)$. For example, in Fig. 2 we see the results for $N_1\times N_2$ $GaAs/Al_{0.7}Ga_{0.3}As$ superlattices: the valence-band maximum is at Γ and the conduction-band minimum for thick GaAs layers ($N_1\geq 8$) is also at Γ. However, for thinner layers ($2\leq N_1<8$) the wave vector of the superlattice conduction-band minimum is at $(2\pi/a_L)(\frac{1}{2},\frac{1}{2},0)$ and the superlattice states associated with this minimum are largely derived from GaAs conduction-band states from near the L point, $(2\pi/a_L)(\frac{1}{2},\frac{1}{2},\frac{1}{2})$, of the bulk Brillouin zone. This is the case because the L point in the bulk, $(2\pi/a_L)(\frac{1}{2},\frac{1}{2},\frac{1}{2})$, is the sum of $(2\pi/a_L)(\frac{1}{2},\frac{1}{2},0)$ and $(2\pi/a_L)(0,0,\frac{1}{2})$, and the bulk point $(2\pi/a_L)(0,0,\frac{1}{2})$ corresponds to $\Gamma=(0,0,0)$ in the superlattice Brillouin zone for N_1+N_2 even. In the thinnest superlattices, $N_1\simeq 1$, the $Al_xGa_{1-x}As$ X point, $(2\pi/a_L)(0,0,1)$, is reflected in the superlattice conduction-band minimum. These conduction-band minima away from the Γ point of the superlattice Brillouin zone have severe consequences for the optical properties of small-period $GaAs/Al_{0.7}Ga_{0.3}As$ superlattices: the superlattices will be indirect-band-gap materials, and hence will be poor candidates for light-emitting devices. For $N_1=1$ in Fig. 2, the band gap is direct and the superlattice conduction-band minimum is at Γ, although this minimum is derived from the X point of the $Al_{0.7}Ga_{0.3}As$ band structure, and so one should expect the direct transitions associated with it to be weaker than those associated with the GaAs Γ minimum for $N_1>8$, for example.

The band gap is somewhat more sensitive to changes of the GaAs layer thickness than to changes in the $Al_xGa_{1-x}As$ layer thickness, as demonstrated in Fig. 3. This sensitivity of the superlattice band gap to the GaAs layer thickness is important for the physics of deep levels in superlattices because, as we shall see below, the deep levels have energies relative to the GaAs valence-band maximum that vary relatively little with the thickness of the GaAs layers. Hence a deep level that is near the conduction-band edge but within the gap in a GaAs quantum well can be "covered up" and autoionized by the conduction-band edge when the GaAs layer thickness is increased and the conduction-band edge descends in energy, while the deep level remains at a relatively constant energy (Fig. 4). Here it is important to remember that we use the new definition of a "deep" level[20] as one that originates from the perturbation caused by the central-cell potential. (This contrasts with the old definition as a level that lies within the band gap by at least 0.1 eV.) As a result there are "deep resonances" that lie in the conduction band, above the band gap. We shall see below that Si in GaAs, although producing only shallow levels in the band gap of bulk GaAs (i.e., its deep levels are all resonances that lie in the conduction band) is a candidate for producing a deep level in the band gap of a $GaAs/Al_xGa_{1-x}As$ superlattice, in the GaAs quantum-well limit. For neutral Si this level, when in the

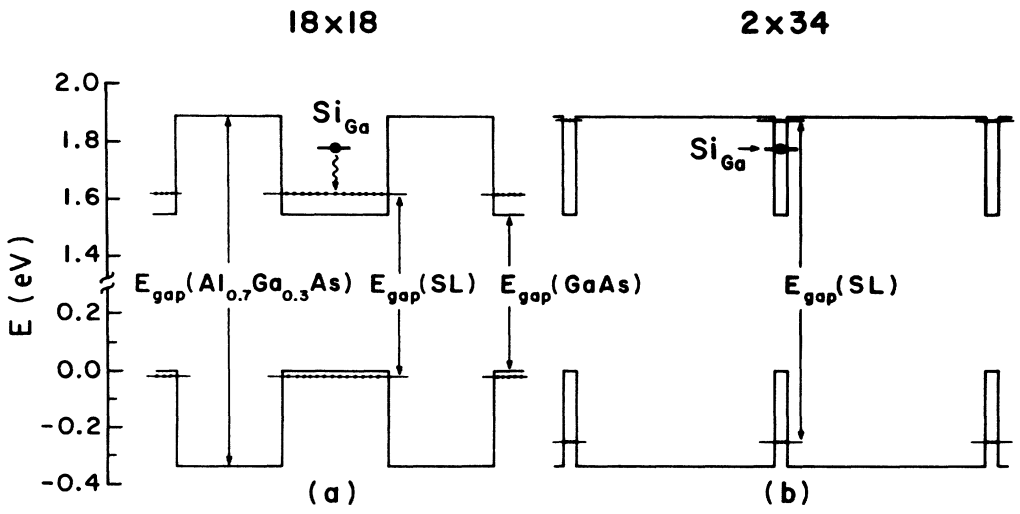

FIG. 1. Illustrating the quantum-well effect on the band gap $E_{gap}(SL)$ of an $N_1\times N_2$ $GaAs/Al_{0.7}Ga_{0.3}As$ superlattice: (a) $N_1=N_2=18$ and (b) $N_1=2$, $N_2=34$. The band edges of the superlattice are denoted by chained lines. For this alloy composition the superlattice gap is indirect for case (b), with the conduction-band edge at $\mathbf{k}=(2\pi/a_L)(\frac{1}{2},\frac{1}{2},0)$. Note the broken energy scale. The zero of energy is the valence-band maximum *of GaAs*.

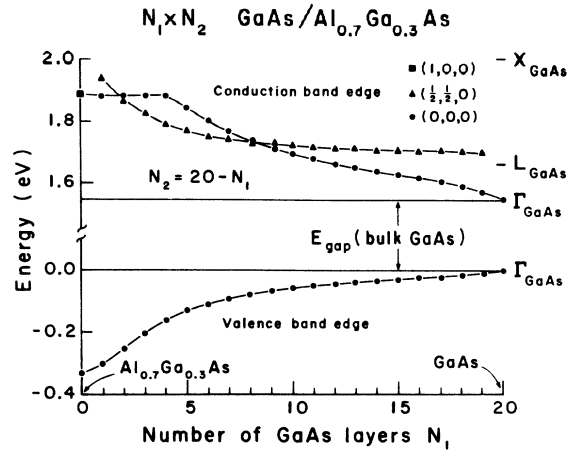

FIG. 2. Predicted energies (in eV) of the superlattice conduction-band minima and valence-band maximum with respect to the valence-band maximum *of bulk GaAs* for a $GaAs/Al_xGa_{1-x}As$ [001] superlattice vs reduced layer thicknesses N_1 and N_2 for various $N_1 \times N_2$ [001] $GaAs/Al_xGa_{1-x}As$ superlattices, with $x=0.7$ and N_1+N_2 fixed to be 20. The calculations are based on the low-temperature band structures of GaAs and $Al_{0.7}Ga_{0.3}As$, with bulk band gaps of 1.55 and 2.22 eV, respectively. The conduction-band minimum of the superlattice is at $(2\pi/a_L)(\frac{1}{2},\frac{1}{2},0)$ for the triangular points, at $\mathbf{k}=\mathbf{0}$ for the circles, and at $(2\pi/a_L)(1,0,0)$ for the rectangle. The superlattice valence-band maximum is at $\mathbf{k}=\mathbf{0}$. Note the broken scale on the ordinate. The positions of the band extrema of bulk GaAs at Γ, L, and X are shown on the right of the figure, at $N_1=20$.

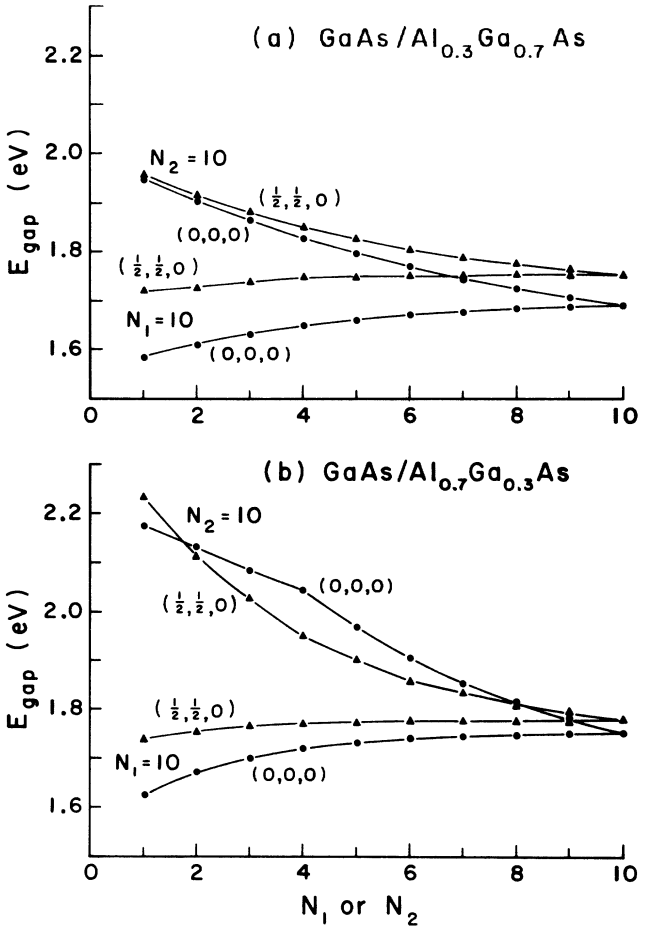

FIG. 3. Predicted fundamental energy band gaps E_{gap} at $\mathbf{k}=\mathbf{0}$ (circles) and $\mathbf{k}=(2\pi/a_L)(\frac{1}{2},\frac{1}{2},0)$ (triangles) of a $(GaAs)_{N_1}(Al_xGa_{1-x}As)_{N_2}$ superlattice as functions of reduced GaAs layer thickness N_1 or $Al_xGa_{1-x}As$ layer thickness N_2 for (a) $x=0.3$ and (b) $x=0.7$. Note that the variation of the gap with decreasing N_2 from, say, 8 to 4, is less than the variation associated with changing N_1 from 8 to 4. Note also that the $\mathbf{k}=\mathbf{0}$ conduction-band extremum of the superlattice in (b) is derived from the X point of the $Al_{0.7}Ga_{0.3}As$ band structure for $N_1<4$ and from the Γ point of the GaAs band structure for $N_1>4$.

fundamental band gap, will be occupied by one electron. When the GaAs layer thickness increases, this level is covered up by the falling conduction-band edge and becomes a resonance. The electron in the resonant level is autoionized and relaxes (e.g., by phonon emission) to the conduction-band edge, where it is a shallow donor electron, donated by the Si. (In the present theory, which neglects the long-ranged Coulomb potential of the donor, the binding energy of a shallow donor is zero; in a more complete theory, the Coulomb potential would trap this electron at zero temperature in a hydrogenic orbit.) A gratifying feature of the band-gap calculation is that we obtain for $N_1=N_2=1$ a fundamental gap of 2.11 eV for a GaAs/AlAs superlattice, in good agreement with the measured value of Ref. 35.

B. Defect levels

The substitutional defect energy levels for sp^3-bonded impurities can be evaluated using the techniques of Hjalmarson *et al.*,[20] as described above for superlattices. When interpreting the predictions, one should remember that the absolute energy levels predicted by this theory have a theoretical uncertainty of a few tenths of an eV. This is, of course, comparable with the uncertainties of the other sophisticated theories of deep levels that have been presented to date.[36] Nevertheless, the theoretical uncertainty is a significant fraction of the band-gap energy, and so one must not use the theory in a futile attempt to predict absolute energy levels with high precision. Rather, the theory should be employed to understand the chemical trends in the deep energy levels, to study qualitative changes in level structures (such as a deep resonance descending into the fundamental band gap—the shallow-deep transition), or to suggest experiments for testing hypotheses about impurity states. One of the reasons that the Hjalmarson model[20] has been so successful is that the tight-binding Hamiltonian[25] has been constructed with manifest chemical trends in its parameters, following ideas developed originally by Harrison.[37] Earlier theories sometimes obtained tight-binding parameters by performing least-squares fits to the band structures of the semiconductors being studied. Such fits, while having

given impressive band structures, often lacked the essential chemistry that determines deep levels, and, as a result, those theories have not been as successful as the Hjalmarson theory. Indeed, because the Hamiltonian employed in the Hjalmarson theory has manifest chemical trends and also has (by construction) the correct band gaps, the Hjalmarson method is comparably accurate with far more cumbersome pseudopotential theories of deep levels.[36,38]

1. *Dependence on layer thickness*

Figure 4 displays the dependence on GaAs reduced layer thickness N_1 of the deep Ga-site A_1 level of a Si impurity[31] *in the middle of a GaAs layer* in a $GaAs/Al_{0.7}Ga_{0.3}As$ superlattice. As the size, N_1, of the GaAs layer shrinks, the *deep levels remain relatively constant in energy* with respect to the GaAs valence-band maximum, while the conduction-band edge of the superlattice increases in energy—progressively uncovering the once-resonant deep level of Si and converting this shallow donor impurity into a deep trap.[39] This shallow-deep transition as a function of GaAs well size N_1, to our knowledge, has not been anticipated in the literature—and has consequences for $GaAs/Al_xGa_{1-x}As$ superlattice and quantum-well devices, because it implies that the most common dopant, Si, may become a deep electron trap rather than a shallow donor in GaAs.

Also note (Fig. 4) that when Si in a GaAs quantum well becomes a deep impurity with its deep level in the fundamental gap of the superlattice, this level (with respect to the GaAs valence-band maximum) generally lies at a higher energy than the bulk GaAs band gap, at lower energy than the Si deep level in an $Al_xGa_{1-x}As$ layer, and below the superlattice and bulk $Al_xGa_{1-x}As$ alloy conduction-band edges. Because Si in an $Al_xGa_{1-x}As$ layer lies at higher energy than Si in a GaAs layer, it is possible to move the conduction-band edge up by reducing the width of the GaAs layers and to achieve a situation such that Si in a GaAs layer is a deep level, but that Si in an $Al_xGa_{1-x}As$ layer is a shallow donor with respect to the superlattice (but not with respect to bulk $Al_xGa_{1-x}As$) because its deep level lies above the superlattice conduction-band edge, but below the bulk $Al_xGa_{1-x}As$ conduction-band edge. In the more common case for very thin GaAs layers, Si in both GaAs and $Al_xGa_{1-x}As$ layers will produce deep levels below the superlattice conduction-band edge; that is, since the superlattice band edge lies below the $Al_xGa_{1-x}As$ band edge, for Si to be deep in a thin GaAs layer requires Si to be a deep level in bulk $Al_xGa_{1-x}As$ as well. Because of this requirement, and the fact that Si successfully modulation-dopes $GaAs/Al_xGa_{1-x}As$ superlattices for $x<0.3$ (suggesting that Si is a shallow donor in, for example, $Al_{0.2}Ga_{0.8}As$), we doubt that the shallow-deep transition as a function of N_1 will be observable in $GaAs/Al_xGa_{1-x}As$ for $x\leq 0.2$. For $x>0.3$, however, Si in bulk $Al_xGa_{1-x}As$ is almost certainly a deep level,[8] modulation doping with Si in $GaAs/Al_xGa_{1-x}As$ superlattices should require thermal activation or tunneling (presumably because Si in an $Al_xGa_{1-x}As$ layer is a deep impurity, not a shallow donor), and the predicted shallow-deep transition for Si in a GaAs layer as a function of GaAs layer thickness should occur.

Because of uncertainties in the theory, we cannot estimate with precision the layer thickness N_1 at which the Si level in GaAs should undergo the shallow-deep transition. Based on the general structure of the curves of Fig. 4, it probably occurs for $N_1\simeq 6$ and a GaAs layer thickness of order $\simeq 17$ Å or less.

A similar analysis can be made of the behavior of other

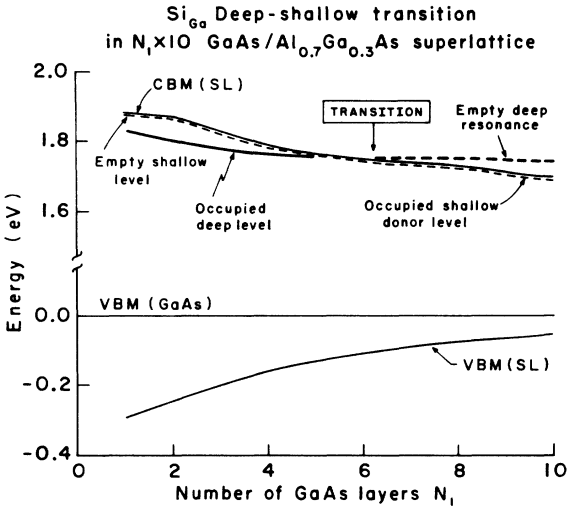

FIG. 4. Illustrating the deep-to-shallow transition as a function of GaAs layer thickness N_1 in a $GaAs/Al_xGa_{1-x}As$ $N_1\times 10$ superlattice (SL) with $x=0.7$ for a Si impurity on a column-III site in the center of a GaAs layer of the superlattice host. The conduction-band minimum (CBM) and valence-band maximum (VBM) are indicated by light solid lines. The Si deep level is denoted by a heavy line, which is solid when the level is in the gap but dashed when the level is resonant with the conduction band. The deep level in the band gap for $N_1<6$ is covered up by the conduction band as a result of changes in the host for $N_1>6$. The impurity's deep level lies in the gap for $N_1<6$ and is occupied by the extra Si electron; the Si, in this case, is thus a "deep impurity." For $N_1>6$ the deep level lies above the conduction-band edge as a resonance. The daughter electron from the Si impurity which was destined for this deep level is autoionized, spills out of the deep resonance level, and falls to the conduction-band edge (light solid line) where it is subsequently bound (at low temperature) in a shallow level associated with the long-ranged Coulomb potential of the donor (indicated by the short-dashed line). It is important to realize that *both* the deep level and the shallow levels coexist and are distinct levels with qualitatively different wave functions. The issue of whether an *impurity* is "deep" or "shallow" is determined by whether or not a deep level associated with the impurity lies in the band gap. The computed deep-shallow transition occurs for $N_1\simeq 6$ layers. While the qualitative physics is completely reliable, it is possible that the transition layer thickness may differ somewhat from $N_1=6$ in real superlattices. The predicted fundamental band gap of the superlattice is indirect for $1<N_1\leq 8$. All energies are with respect to the valence-band maximum *of GaAs*.

impurities,[16] for example, N in GaAs. Nitrogen has a resonant state in the conduction band of GaAs. We have predicted that this resonant state can be driven out of the conduction band into the band gap by hydrostatic pressure,[40] an effect that has been observed by Wolford *et al.*[41] and Zhao *et al.*[42] Here we predict that N in GaAs layers of a $GaAs/Al_{0.7}Ga_{0.3}As$ superlattice will have an impurity state in the band gap if the thickness of the GaAs layers is thin enough, for example, ≤ 48 Å or 17 molecular layers.

2. *As vacancy levels*

Figure 5 displays the deep energy levels in the band gap of an As vacancy in an $N_1=N_2=10$ $GaAs/Al_{0.7}Ga_{0.3}As$ superlattice, as a function of β, the z component of the position of the vacancy in the superhelix or superslab. A vacancy is simulated here by letting the defect-potential elements V_s and V_p at the vacancy site approach infinity, making the defect into an "atom" with infinite orbital energies, and thereby decoupling it from the host by virtue of the fact that all energy denominators in a perturbation expansion are infinite.[43] Several features of the results in Fig. 5 are worth noting: The valence-band maximum of the superlattice splits, with the p_z-like edge moving to lower energy, owing to its lighter effective mass. Near an interface ($\beta=0$, 20, or 40) the p-like T_2 bulk As vacancy level splits into three levels, a_1, b_1, and b_2. For any point defect, one of the b_1 or b_2 levels corresponds to a p-like level with its orbital composed of hybrids directed toward the GaAs layer and has an energy almost the same as the bulk GaAs T_2 level; the other is composed of hybrids directed toward the $Al_xGa_{1-x}As$ and is virtually an $Al_xGa_{1-x}As$ T_2 level. The b_1 and b_2 levels reverse ordering from $\beta=0$ to $\beta=20$ (because of the defined orientation of the x and y axes), and a_1 lies between them in most cases such that the splitting of the host valence-band edge can be neglected. The splittings between the b_1 and b_2 levels at the interface are small, of order 0.1 eV, and become negligible when the vacancy is more than three or so atomic layers from the interface (a fact noted first for deep levels near surfaces by Daw and Smith[44]). The splitting between the a_1 level and the b_1 and b_2 levels is comparably small, but may not vanish even if the defect is distant from the interface, as a result of the splitting of the valence-band edge in the superlattice and the resulting changes of the host spectral density.

The energy of a deep level is determined by a balance between the conduction-band states, which push the level down in energy, and the valence-band states, which repel it upward. Since the GaAs valence-band maximum is almost at the same energy as the valence-band maximum for the 10×10 $GaAs/Al_{0.7}Ga_{0.3}As$ superlattice, the conduction band has the primary influence on the change of the energies of the As-vacancy deep level from bulk

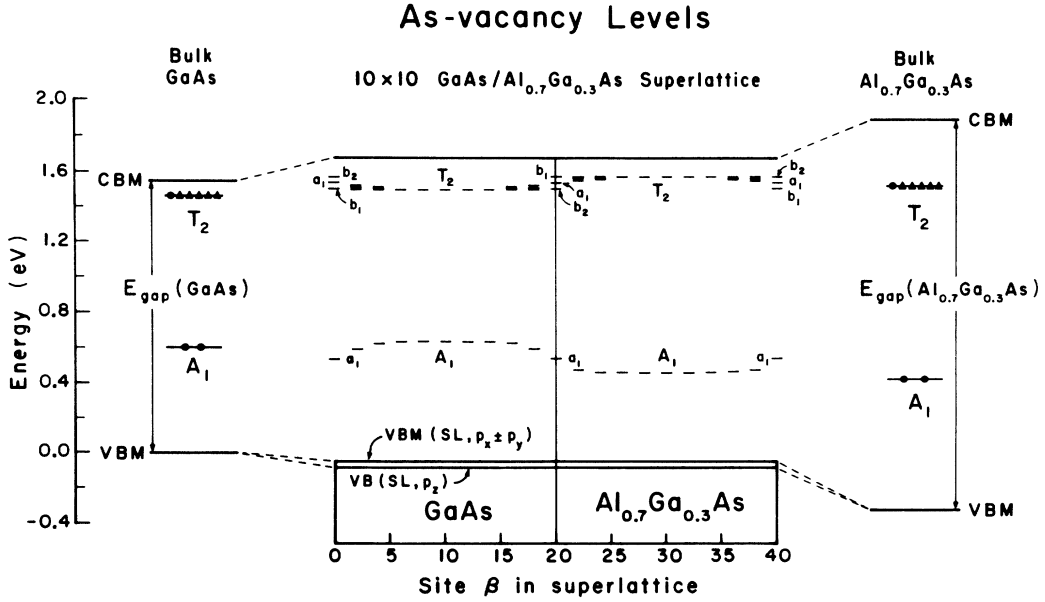

FIG. 5. Predicted energy levels of an As vacancy in a $(GaAs)_{10}/(Al_{0.7}Ga_{0.3}As)_{10}$ superlattice, as a function of β, the position of the vacancy (even values of β correspond to As sites). Note the splitting of the T_2 levels at and near the interfaces ($\beta=0$, 20, and 40), and that the T_2-derived vacancy levels lie at higher energy in an $Al_{0.7}Ga_{0.3}As$ layer than in a GaAs layer. The b_1 and b_2 ordering changes at successive interfaces. The zero of energy is the valence-band maximum of bulk GaAs, and the corresponding valence-band (VBM) and conduction-band (CBM) edges and deep levels in bulk GaAs and bulk $Al_{0.7}Ga_{0.3}As$ are given to the left and right of the central figure, respectively. The top of the central figure is the conduction-band edge of the superlattice, and the bottom corresponds to the split valence band in the superlattice—the valence-band maximum of the superlattice being of b_1 or b_2 symmetry ($p_x\pm p_y$) and the split-off a_1 (p_z) band maximum lying 0.062 eV lower in energy. The A_1 level in the $Al_xGa_{1-x}As$ layer of the superlattice is lower than the corresponding level in the GaAs layer because of the band offset of 0.334 eV. The electron (hole) occupancies of the deep levels in bulk GaAs and bulk $Al_{0.7}Ga_{0.3}As$ are denoted by solid circles (open triangles).

GaAs to a GaAs layer in the superlattice, and the levels move up in energy because the conduction-band minimum does. In going from an $Al_{0.7}Ga_{0.3}As$ layer in the superlattice to bulk $Al_{0.7}Ga_{0.3}As$, the levels move down in energy, because the valence-band maximum moves down. (The valence-band maximum is T_2-like.) The T_2 As vacancy levels lie at somewhat higher energy in an $Al_xGa_{1-x}As$ layer than in a GaAs layer, owing to the fact that Al is more electropositive than Ga. The A_1 bulk As-vacancy level in $Al_xGa_{1-x}As$ is slightly shifted at the interface, and is at lower energy in an $Al_xGa_{1-x}As$ layer than in a GaAs layer because the band offset causes the nearest A_1 states in the valence band to lie at lower energy than in the superlattice. The T_2 level in GaAs ($Al_xGa_{1-x}As$) is both split in the superlattice and, on the average, is shifted up (down) in energy at the interface. Because of the band offset, the A_1 level for the As vacancy in GaAs ($Al_xGa_{1-x}As$) moves down (up) at the interface. Still another effect does influence the relative ordering of the a_1, b_1, and b_2 levels: As the impurity approaches the interface in GaAs (but not in $Al_xGa_{1-x}As$) its wave function suffers quantum confinement and its energy levels shift—and the shifts for b_1 and b_2 levels are generally different from those for a_1 levels because the a_1 valence-band edge in the 10×10 superlattice lies lower by 0.062 eV than the b_1 and b_2 edges. The conduction-band minimum in the 10×10 superlattice has s symmetry and does not split.

For the neutral vacancy, the A_1-derived deep level is filled by two electrons, and one electron occupies the lowest of the T_2-derived states.

Similar behavior to that found for the As-vacancy levels is to be expected for all sp^3-bonded deep impurity levels in GaAs/$Al_xGa_{1-x}As$ superlattices, although the issue of whether a specific deep level lies in the fundamental band gap or not depends on the defect potential for that impurity and on N_1, N_2, and x.

3. *Cation-vacancy levels*

The A_1 bulk levels for a Ga vacancy in GaAs and for a cation vacancy in $Al_xGa_{1-x}As$ all lie very deep in the host valence bands and are not near the fundamental band gap, either in the bulk or at an interface of a GaAs/$Al_xGa_{1-x}As$ superlattice.

The T_2-derived cation-vacancy levels produce deep levels near the valence-band maxima of bulk GaAs, bulk $Al_xGa_{1-x}A$,[45,46] and the superlattice (see Fig. 6). In the Hjalmarson-type theory, the uncertainty in the predictions of absolute energies is typically a few tenths of an

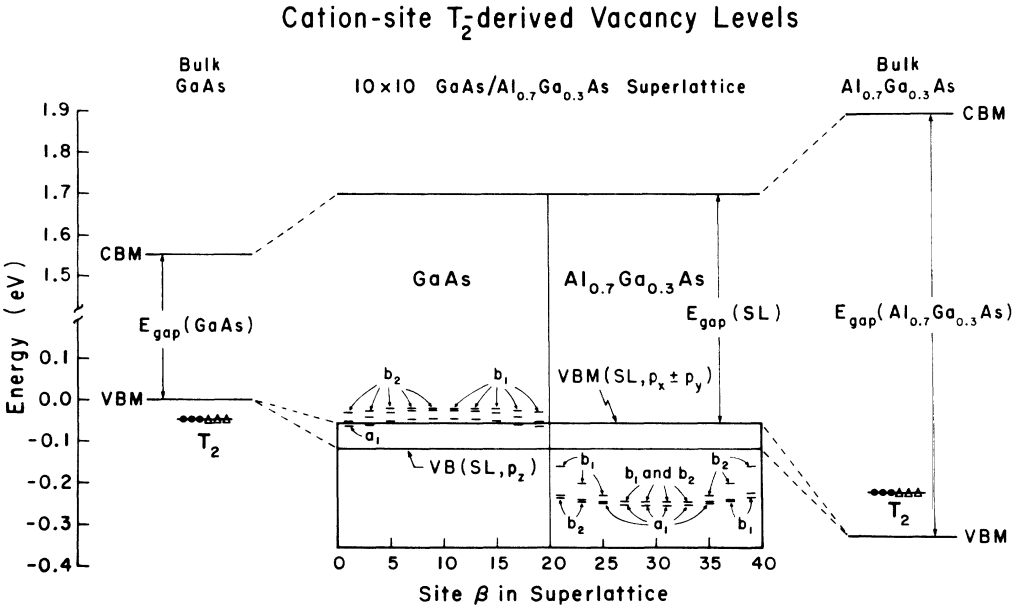

FIG. 6. Predicted T_2-derived vacancy levels of a cation vacancy in a $(GaAs)_{10}/(Al_{0.7}Ga_{0.3}As)_{10}$ superlattice, as a function of site index β, the position of the vacancy. The zero of energy is the valence-band edge of bulk GaAs, and the corresponding valence- and conduction-band edges and deep levels in bulk GaAs and bulk $Al_{0.7}Ga_{0.3}As$ are given to the left and right of the central figure, respectively. The top of the central figure is the conduction-band edge of the superlattice, and the two bottom lines correspond to the b_1- and b_2-symmetric [$(p_x \pm p_y)$-like] valence-band maxima and the split a_1 (p_z-like) edge below it. Electrons occupying the bulk levels are denoted by solid circles. Holes are denoted by open triangles. When, as in bulk GaAs, the holes are initially in levels *below the valence-band maximum*, they bubble up to the valence-band maximum where the long-ranged Coulomb potential can trap them into shallow acceptor levels (not shown). The cation vacancy in bulk GaAs and in an $Al_{0.7}Ga_{0.3}As$ layer in the superlattice is predicted to be a triple shallow acceptor, providing three such holes to the valence band. In bulk $Al_{0.7}Ga_{0.3}As$ and in a GaAs layer of the superlattice, neutral cation vacancies are predicted to produce deep traps for either electrons or holes. In the superlattice, the lowest-energy level is often of a_1 symmetry, and the highest is typically either of b_1 or b_2 symmetry, but exceptions to this rule do occur, as indicated on the figure.

eV and tends to be somewhat larger for the T_2 levels than for the A_1 levels. Therefore, in what follows, the reader should not interpret our predictions for the cation vacancy too literally or too quantitatively. Rather, the predictions illustrate the very interesting properties of a cation-site deep T_2 level that lies near but below the valence-band maximum of GaAs. Since this defect never lies at the interface (which, by definition in a $GaAs/Al_xGa_{1-x}As$ superlattice, is at an As layer), its level splittings are smaller (<0.05 eV) than the interfacial anion vacancy's splittings. In bulk GaAs, the T_2 cation-vacancy level is predicted[20,46] to lie $\simeq 0.03$ eV below the valence-band maximum. In bulk $Al_{0.7}Ga_{0.3}As$, the predicted vacancy level is in the gap, 0.11 eV above the $Al_{0.7}Ga_{0.3}As$ valence-band maximum. Near a $GaAs/Al_xGa_{1-x}As$ interface, the T_2 cation-vacancy level splits into a_1, b_1, and b_2 sublevels. For $x \simeq 0.7$ some or all of these sublevels may lie in the gap of the superlattice.

If the predictions are taken literally, then near the interface the cation vacancy produces a very interesting level structure, depending on the site of the vacancy. To begin with, in a GaAs layer the b_1 and b_2 vacancy levels lie in the gap of the superlattice, but in an $Al_{0.7}Ga_{0.3}As$ layer the vacancy levels are resonant with the valence band. This is due mainly to the band offset and the fact that, roughly speaking, the deep levels do not move (much), whereas the valence-band edges do, as one goes from bulk GaAs to the superlattice to bulk $Al_{0.7}Ga_{0.3}As$. The b_1 and b_2 levels in a GaAs layer lie typically $\simeq 0.03$ eV above the a_1 level, when we might have expected the a_1 level to lie between them. This expectation is not met because the T_2 levels are near the valence-band maximum and, in the superlattice, the T_2-like valence-band maximum is split into a_1 and b_1 and b_2 edges. Hence the a_1 valence-band edge has a stronger quantum-well-confinement effect: the band edge for a_1 (p_z-like) states lies 0.062 eV below the edge for b_1 and b_2 states. The a_1 defect states lie lower because the valence-band states that repel them are at lower energy in the superlattice. The largest splitting between b_1 and b_2 states is of order $\simeq 0.02$ eV, much smaller than the ($\simeq 0.1-0.2$)-eV splittings deduced from the anion vacancy—because the cation vacancy always lies at least one layer from an interface. In particular, the p_z-like a_1 level decreases in energy as the vacancy moves from the center of the GaAs layer toward the interface. The initial decrease is due to quantum-well confinement, and begins when the vacancy wave function significantly overlaps the $Al_{0.7}Ga_{0.3}As$. However, as the vacancy becomes quite close to the interface, its wave function penetrates thoroughly into the $Al_{0.7}Ga_{0.3}As$ layer and feels the electropositivity of the

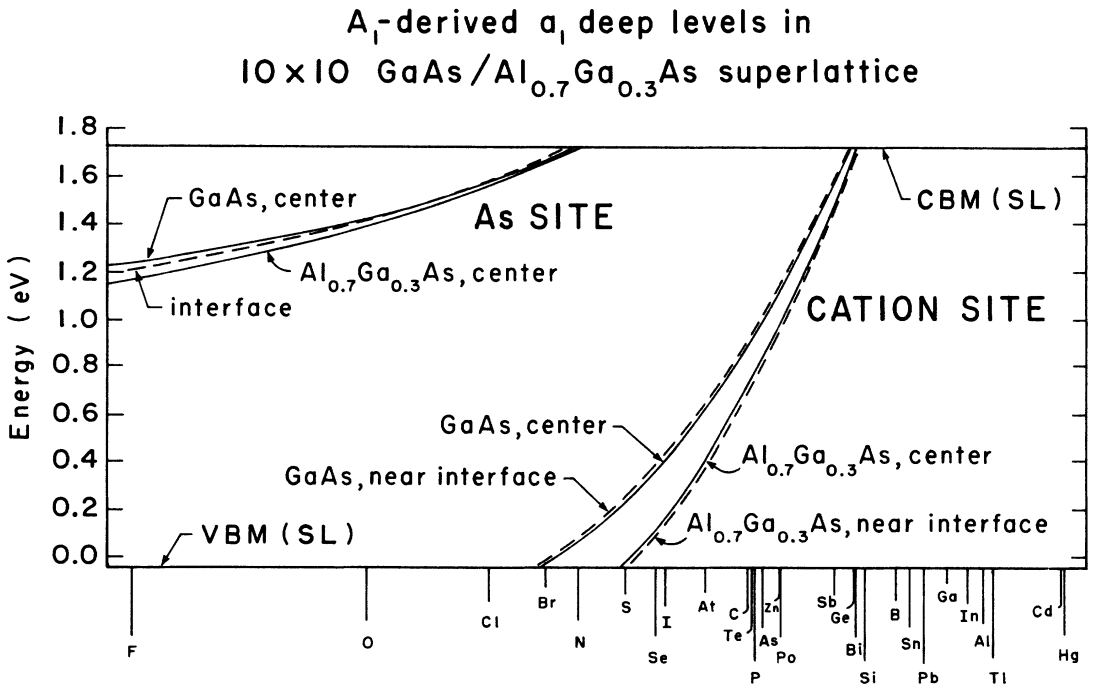

FIG. 7. Predicted energies of A_1-derived s-like a_1 deep levels of the indicated defects (Ref. 47) for a $GaAs/Al_{0.7}Ga_{0.3}As$ superlattice with $N_1 = 10$ GaAs layers and $N_2 = 10$ $Al_{0.7}Ga_{0.3}As$ layers in its unit supercell. The dashed lines denote the predictions for defects at or near a $GaAs/Al_{0.7}Ga_{0.3}As$ interface: in the $\beta = 0$ layer for the interface, levels for As-site defects (upper left-hand corner), and, in the $\beta = 1$ and $\beta = 21$ layers adjacent to interface layers, for Ga-site defects (in GaAs) and cation-site defects in $Al_{0.7}Ga_{0.3}As$, respectively (lower right-hand corner). The solid lines denote the same levels for defects at or near the center of GaAs and $Al_{0.7}Ga_{0.3}As$ layers, respectively. In viewing this figure, remember that the theory is not precise, but that the general shape of the figure is reliable. The zero of energy is the valence-band maximum *of bulk GaAs*. The valence- and conduction-band edges of the superlattice are denoted VBM(SL) and CBM(SL), respectively.

Al. If the valence-band offset were smaller, say 0.2 eV, then this effect would cause the level to increase in energy near the interface.

The neutral Ga vacancy in the bulk of GaAs (assuming its deep level lies in the valence band) is a triple acceptor (Fig. 6). (A Ga vacancy is created by adding three holes—to remove the three Ga electrons—and letting the defect potential become infinite.[43]) Consider this vacancy at the near-interfacial site $\beta=1$ in a GaAs layer of the superlattice; its levels, in order of decreasing energy, are b_2, b_1, and a_1. In all of the cases of Fig. 6, the cation vacancy is either a triple shallow acceptor or a deep trap for both an electron and a hole, having at least one partially filled deep level in the gap. If it were the case that a cation vacancy near an interface had only one of its sublevels in the gap and two sublevels resonant with the valence band of the superlattice, then the vacancy would be a single acceptor, because only three electrons are available for four spin orbitals: the hole in the fourth spin orbital would "bubble up" to the valence-band maximum. Relatively small amounts of lattice relaxation or charge-state splittings of the defect levels could alter the predictions. Nevertheless, we think that studies of the character of the Ga-vacancy wave function in $GaAs/Al_xGa_{1-x}As$ superlattices are warranted—and could possibly reveal this shallow-deep transition in the character of the cation vacancy.

4. *Deep levels of sp^3-bonded impurities*

The predicted deep energy levels of substitutional sp^3-bonded impurities in a $GaAs/Al_{0.7}Ga_{0.3}As$ superlattice are given in Figs. 7 and 8 for a superlattice with $N_1=N_2=10$.[31,47] These levels' energies E are obtained by solving the secular equation (17) with Hjalmarson's defect potential V slightly modified.[31] In these figures we display results for impurities at or near a $GaAs/Al_{0.7}Ga_{0.3}As$ interface and near the center of the GaAs and $Al_{0.7}Ga_{0.3}As$ layers.

For the A_1- or s-like a_1 levels on the As site (Fig. 7), most interfacial impurities have energy levels roughly midway between the levels for impurities near the center of the GaAs and the $Al_xGa_{1-x}As$ layers. There are two types of cation sites: Ga (in GaAs) and Al_xGa_{1-x} (in

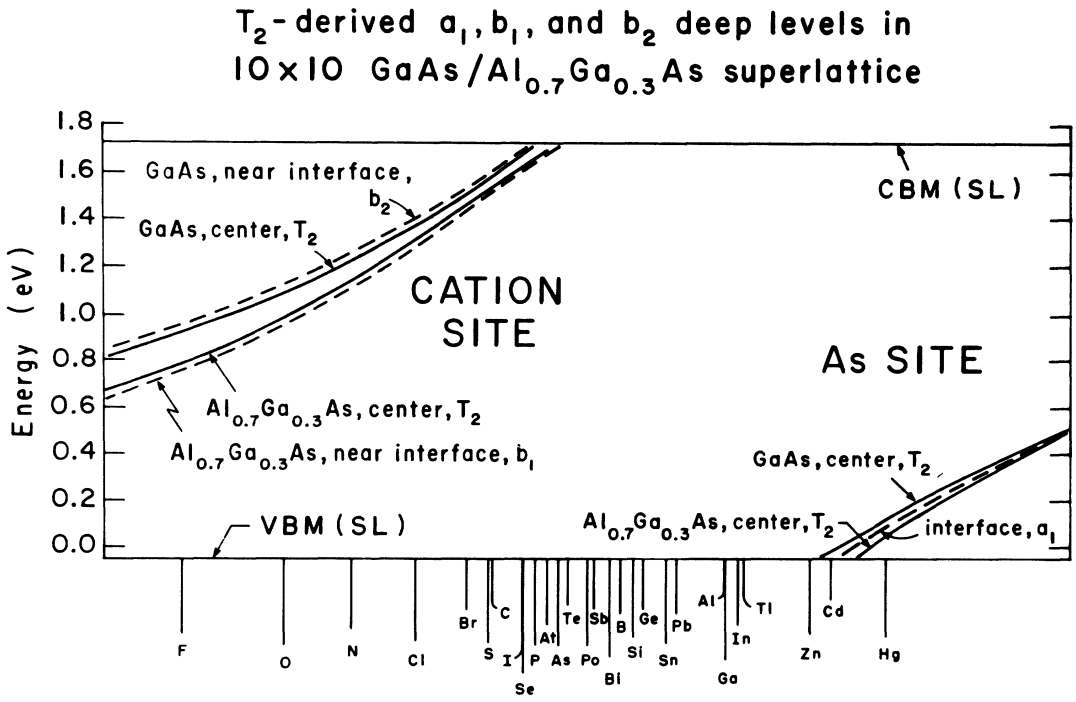

FIG. 8. The predicted T_2-derived deep levels for the indicated defects (Ref. 47) in a $(GaAs)_{10}/Al_{0.7}Ga_{0.3}As)_{10}$ superlattice. For As-site defects (lower right-hand corner) the two solid lines correspond to T_2-derived b_1 levels (which are almost degenerate with b_2 levels) in the center of GaAs and $Al_{0.7}Ga_{0.3}As$ layers. The corresponding T_2-derived a_1 levels lie slightly (of order 0.01 eV) below the b_1 and b_2 levels and are not shown. The dashed line is an interfacial $\beta=0$ a_1 level. The corresponding b_2 level (not shown) is nearly degenerate with it, and the b_1 level (not shown) is above it of order 0.01 eV. For cation-site defects (upper left-hand corner), the solid lines correspond to T_2-derived b_1 levels (which are almost degenerate with b_2 and a_1 levels not shown). The dashed lines correspond to interfacial levels for site $\beta=19$ (in GaAs) of b_2 symmetry and for site $\beta=21$ of b_1 symmetry. The $\beta=19$ a_1 and b_1 levels are almost degenerate with the T_2 levels of defects in the center of GaAs and are not shown. Similarly, the $\beta=21$ ($Al_{0.7}Ga_{0.3}As$) a_1 and b_2 (which are polarized perpendicular to the interface) interfacial levels are not shown. Near the $\beta=0$ interface, the b_1 and b_2 levels are interchanged. Simply stated, the levels b_1 or b_2 are split off from the bulk T_2 energy (in the material occupied by the defect), and the remaining two levels (almost) are at the T_2 bulk energy. The zero of energy is the valence-band maximum *of bulk GaAs*. The valence- and conduction-band edges of the superlattice are denoted VBM(SL) and CBM(SL), respectively.

$Al_xGa_{1-x}As$); the cation-site defects near the GaAs/$Al_xGa_{1-x}As$ interface have nearly the same deep levels as defects at the center of the layers—because those defects are at least one layer distant from the interface (which coincides with an As layer), and hence are only weakly perturbed by the atoms on the other side of the interface.

The T_2-derived levels in the GaAs layer (Fig. 8) are split when they lie near or at the interface. These are dangling-bond-p-like levels, and the p orbitals composed of hybrids oriented most toward the interface are split most [b_1 or (p_x+p_y)-like and a_1 or p_z-like on the Ga site; b_2 or (p_x-p_y)-like and a_1 at the As site], whereas the orbital directed away from the interface is least perturbed and normally has a level closest to that of the bulk T_2 level. The same physics hold for defects in the $Al_xGa_{1-x}As$ layer (Fig. 8), but the signs of the splittings and the orderings of b_1, a_1, and b_2 levels are normally reversed.

In general, three factors influence the relative positions of deep levels in GaAs and $Al_xGa_{1-x}As$ layers. (i) The more electropositive character of Al with respect to Ga pushes levels up in energy, so that the same defect has a tendency to exhibit higher-energy deep levels in $Al_xGa_{1-x}As$ than in GaAs. (See the T_2-derived As-vacancy levels in Fig. 5.) (ii) However, the Al also widens the band gap, causing a band offset, and rearranging the spectral distribution of host states somewhat (differently for the b_1 and b_2 states than for the a_1 states)—which often has the opposite effect on those impurity levels most affected by the host states near the valence-band maximum. (See the A_1-derived As-vacancy levels in Fig. 5.) (iii) In addition to the electropositivity and band-gap-widening effects, there is a quantum-well-confinement effect. Impurities in GaAs close enough to an $Al_xGa_{1-x}As$ layer that their wave functions overlap the $Al_xGa_{1-x}As$ barrier will experience level shifts due to confinement (that depend on the symmetry of the level). States near and above the conduction-band minimum with considerable conduction-band character are expected to move up in energy and valence-band states should move down due to confinement (see Fig. 6). The confinement effects should be more severe for a_1 states than for b_1 or b_2 states, due to the fact that their wave functions are polarized in the superlattice growth direction.

5. *Dependence on alloy composition*

In Fig. 9 we show our predictions for the A_1-symmetric deep level of cation-site Si (Ref. 31) in bulk $Al_xGa_{1-x}As$ as a function of x, which are similar to those first obtained by Hjalmarson.[48]

Figure 10, in comparison with Fig. 9, illustrates that a Si impurity in a GaAs/$Al_xGa_{1-x}As$ superlattice with $N_1=N_2$ may *not* produce a deep level in the superlattice band gap, although the same impurity in the alloy obtained by disordering the superlattice, $Al_{(x/2)}Ga_{1-(x/2)}As$, does produce a deep level in the gap of the alloy. To see this, consider $x<0.5$, for which the Si theoretical level does not lie in the gap of the 2×2 GaAs/$Al_xGa_{1-x}As$ superlattice. For $x=0.25$ the Si level is in the gap of the alloy, however.

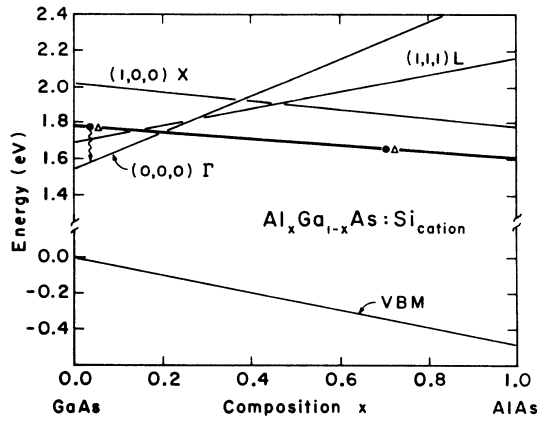

FIG. 9. Chemical trends with alloy composition x in the energies (in eV) of principal conduction-band edges Γ, L, and X, and the valence-band maximum of the alloy with respect to the valence-band maximum *of GaAs*, in the alloy $Al_xGa_{1-x}As$, as deduced from the Vogl model (Ref. 25). Also shown is the predicted energy of the A_1-symmetric cation-site deep level of Si (heavy line), similar to the predictions of Hjalmarson (Refs. 31 and 48). The Vogl model is known to obtain very little band bending. Moreover, the L minimum for $x\simeq0.45$ is known to be at a bit too low an energy in this model. When the deep level of neutral Si lies below the conduction-band minimum, it is occupied by one electron (solid circle) and one hole (open triangle). When this level is resonant with the conduction band, the electron spills out and falls (wavy line) to the conduction-band minimum, where it is trapped (at zero temperature) in a shallow donor level (not shown).

This situation is much more common in larger-period superlattices,[13] where the band edge of the superlattice is almost the band gap of the small-band-gap material (GaAs) (see Fig. 1). To a good approximation, if an im-

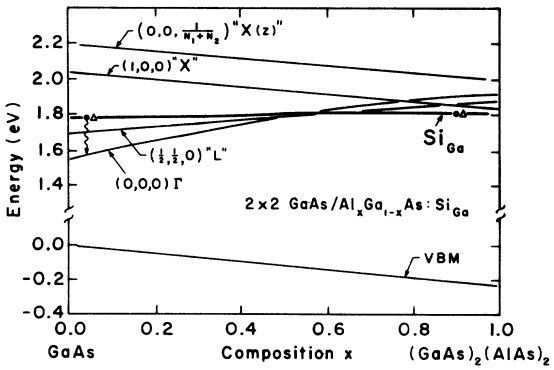

FIG. 10. Chemical trends with alloy composition x in the energies (in eV) of principal conduction- and valence-band extrema of a $(GaAs)_2/(Al_xGa_{1-x}As)_2$ superlattice, with respect to the valence-band maximum *of GaAs*. Compare with Fig. 9 for the alloy. The superlattice wave vectors of the minima are $\mathbf{k}=0$, $\mathbf{k}=(2\pi/a_L)(\frac{1}{2},\frac{1}{2},0)$, which has states derived from the L point of the bulk Brillouin zone, and the points derived from the bulk X point: $(2\pi/a_L)(0,0,(N_1+N_2)^{-1})$, which is p_z-like, and $(2\pi/a_L)(1,0,0)$, which is p_x- and p_y-like.

purity[20] (i) produces a deep level in the gap when the impurity lies in the large-band-gap bulk material ($Al_xGa_{1-x}As$), and (ii) has its corresponding deep level resonant with the host bands when the impurity occupies a site in the small-band-gap bulk material (GaAs), then the impurity's deep level will not lie in the gap of the large-period superlattice for the case that the impurity occupies a site in a small-band-gap (GaAs) layer. Thus in an 18×18 $GaAs/Al_{0.7}Ga_{0.3}As$ superlattice (Fig. 1), Si on a Ga site in a GaAs layer has its A_1-symmetric deep level in the conduction band of the superlattice, and so is a shallow donor. However, in the corresponding alloy with $x=0.35$ (Fig. 9) the cation-site Si level lies within the fundamental band gap and is a deep trap. Similar physics holds for other defects. This physics might be the origin of the improved transport characteristics of GaAs/AlAs superlattices over $Al_{0.5}Ga_{0.5}As$ alloys, as observed by Fujiwara *et al.*[13]

6. *Fluctuations*

For some time it has been known that fluctuations in alloy composition x of $Al_xGa_{1-x}As$ can cause normally shallow donors such as Si (for $x<0.3$) to produce deep levels in regions where the Al mole fraction is considerably larger than the average value x. Here we have shown that in thin quantum wells of GaAs in $GaAs/Al_xGa_{1-x}As$ superlattices for $x>0.3$ the Si can produce deep levels as well. Thus fluctuations in layer thickness can produce previously unanticipated deep traps. Since deep-level wave functions have large amplitudes only within a radius of $\simeq5$ Å of the impurity, a fluctuation in GaAs layer thickness (in the z direction) down to, say, 20 Å, occurring within a small circle of radius 5 Å in the x-y plane, would lead to Si deep levels in that region. Hence, special care may be necessary during superlattice growth to prevent nonuniformities in layer thickness, which could lead to such deep-level formation.

7. *Relationship between cation-site Si and the DX center*

For some time the technologically important native defect *DX* in $Al_xGa_{1-x}As$ has been the subject of discussion, with Lang[6] first proposing that it is a donor-vacancy complex, and Hjalmarson[4,17,20,49] setting forth the model of a Si impurity on a cation site. Clearly, the Si center discussed here has the energy levels and dependencies on alloy composition x required of a *DX* center. Our opinion is that the *DX* center is normally either a Si impurity, a complex containing a Si impurity (perhaps Si-Si pairs in some cases), or, in some instances, other impurities such as Sn that are similar to Si. The complexes should have spectra very close to the spectra of their constituents.[50] The persistent photoconductivity associated with the *DX* center appears to be best explained by the Hjalmarson-Drummond phonon-coupling model.[4] However, we note that Li *et al.*[51] dispute the Hjalmarson-Drummond conclusion and there remain unanswered questions concerning the *DX* center. We hope that the present work, which shows how the deep levels associated with Si should behave in the superlattice, may help in solving the mysteries surrounding this interesting defect.

IV. SUMMARY

The calculations presented here call into question the common assumption that the character of an impurity in a superlattice will always be the same as in the bulk. We have presented calculations which indicate that the normal shallow dopant Si in GaAs may become a deep trap in a GaAs quantum well of a $GaAs/Al_xGa_{1-x}As$ superlattice. This prediction should be tested for $x\gtrsim0.7$ superlattices, where it is likely to be most reliable.[52]

We have elucidated the physics of deep levels in superlattices, and find splittings of T_2 bulk levels and shifts of A_1 levels of order 0.1–0.2 eV for defects at the interface and less for impurities within two or three atomic planes of an interface. For impurities more distant from an interface the effect of the superlattice is primarily to change the *window of observability* of the deep level: If one imagines the deep levels as being relatively fixed in energy, the role of the superlattice is to provide the band gap; superlattices with small GaAs quantum wells have sufficiently large band gaps that deep levels which are covered up by the bands in bulk GaAs are uncovered and observable in the superlattice.

ACKNOWLEDGMENTS

We are grateful to the U.S. Office of Naval Research (Contract No. N00014-84-K0352) for their generous support. We thank K. Hess for alerting us to the technological importance of this problem, and we have benefited from illuminating conservations with D. Wolford, W. Wang, H. Hjalmarson, and R. Hong.

---

*Permanent address.

[1]L. Esaki and R. Tsu, IBM Research Note RC-2418, 1969 (unpublished).

[2]R. Dingle, H. L. Störmer, A. C. Gossard, and W. Wiegmann, Appl. Phys. Lett. **33**, 665 (1978).

[3]D. K. Maude, J. C. Portal, L. Dmowski, T. Foster, L. Eaves, M. Nathan, M. Heiblum, J. J. Harris, and R. B. Beall, Phys. Rev. Lett. **59**, 815 (1987); M. D. Sturge, Appl. Phys. Lett. **33**, 665 (1978).

[4]H. P. Hjalmarson and T. J. Drummond, Appl. Phys. Lett. **48**, 657 (1986); see also Ref. 5.

[5]J. C. M. Henning and J. P. M. Ansems, Mater. Sci. Forum **10-12**, 429 (1986); Semicond. Sci. Technol. **2**, 1 (1987); A. K. Saxena, Solid State Electron. **25**, 127 (1982).

[6]D. V. Lang and R. A. Logan, Phys. Rev. Lett. **39**, 635 (1977); D. V. Lang, R. A. Logan, and M. Jaros, Phys. Rev. B **19**, 1015 (1979).

[7]T. Ishibashi, S. Tarucha, and H. Okamoto, Jpn. J. Appl. Phys. **21**, 476 (1982).

[8]L. G. Salmon and I. J. D'Haenens, J. Vac. Sci. Technol. B **2**,

197 (1984).
[9]M. Mizuta, M. Tachekawa, H. Kukimoto, and S. Minomura, Jpn. J. Appl. Phys. **24**, L143 (1985).
[10]P. M. Mooney, E. Calleja, S. L. Wright, and M. Heiblum, Mater. Sci. Forum **10**, 417 (1986).
[11]See also, K. J. Malloy, Ph.D. thesis, Stanford University, 1984.
[12]T. Mimura, S. Hiyamizu, T. Fujii, and K. Nambu, Jpn. J. Appl. Phys. **19**, L225 (1980); K. Hess, Physica **117&118B**, 723 (1983); M. Inoue, S. Hiyamizu, M. Inayama, and Y. Inuishi; Jpn. J. Appl. Phys. Suppl. **22-1**, 357 (1983); H. Sakaki, *ibid.* **21**, 381 (1982).
[13]K. Fujiwara, H. Oppolzer, and K. Ploog, Inst. Phys. Conf. Ser. No. 74, 351 (1985); in *Gallium Arsenide and Related Compounds, 1984,* edited by B. de Cremoux (Hilger, Bristol, 1985).
[14]S. Das Sarma and A. Madhukar, J. Vac. Sci. Technol. **19**, 447 (1981).
[15]A preliminary account of this work was given by J. Shen, S. Y. Ren, and J. D. Dow, Bull. Am. Phys. Soc. **30**, 630 (1985). See also Ref. 16.
[16]R.-D. Hong, D. W. Jenkins, S. Y. Ren, and J. D. Dow, Proc. Mater. Res. Soc. **77**, 545 (1987).
[17]A preliminary account was given by H. P. Hjalmarson, Bull. Am. Phys. Soc. **32**, 814 (1987). See also J. W. Farmer, H. P. Hjalmarson, and G. A. Samara, Proc. Mater. Res. Soc. (to be published).
[18]J. S. Nelson, C. Y. Fong, I. P. Batra, W. E. Pickett, and B. M. Klein (unpublished).
[19]M. Lannoo and J. Bourgoin (private communication).
[20]H. P. Hjalmarson, P. Vogl, D. J. Wolford, and J. D. Dow, Phys. Rev. Lett. **44**, 810 (1980); see also W. Y. Hsu, J. D. Dow, D. J. Wolford, and B. G. Streetman, Phys. Rev. B **16**, 1597 (1977), for the concepts that form the foundation of this work.
[21]J. D. Dow, in *Highlights of Condensed Matter Theory,* Proceedings of the International School of Physics "Enrico Fermi," Course 89, Varenna, 1983, edited by F. Bassani, F. Fumi, and M. P. Tosi (Societa Italiana di Fisica, Bologna/North-Holland, Amsterdam, 1985), pp. 465 *et seq.*
[22]S. Y. Ren, W. M. Hu, O. F. Sankey, and J. D. Dow, Phys. Rev. B **26**, 951 (1982).
[23]S. Y. Ren, Sci. Sin. **27**, 443 (1984).
[24]The tight-binding formalism we use here is hybrid based. For bulk semiconductors the hybrid-based tight-binding formalism is equivalent to the widely used atomic-orbital-based tight-binding formalism. However, for superlattices these two formalisms are different: Because the atomic-orbital-based tight-binding parameters are obtained by fitting to the band structure of bulk GaAs and bulk AlAs, the tight-binding parameters for the As atom at $\beta=0$ (which is considered to be an As atom in GaAs) are usually different from the corresponding tight-binding parameters for the atom at $\beta=2N_1$ (which is considered to be an As atom in AlAs). However, both of these As atoms are interfacial As atoms and physically they are completely equivalent to each other. The way we correct for this problem is that we assign the tight-binding parameters to bonds rather than to atoms: We consider the hybrids h_1 and h_4 of the As atoms at $\beta=0$ to be hybrids of GaAs, while h_2 and h_3 are taken to be AlAs hybrids. Similarly, h_2 and h_3 of the As atom at $\beta=2N_1$ are considered to be hybrids in GaAs, and h_1 and h_4 are AlAs hybrids. We believe that this properly accounts for the correct physics and the nature of interfacial bonds.
[25]P. Vogl, H. P. Hjalmarson, and J. D. Dow, J. Phys. Chem. Solids **44**, 365 (1983).
[26]D. J. Wolford, T. F. Kuech, J. A. Bradley, M. A. Grell, D. Ninno, and M. Jaros, J. Vac. Sci. Technol. B **4**, 1043 (1986).
[27]In our model, which uses low-temperature band gaps, we take the valence-band offset for $Al_{0.7}Ga_{0.3}As$ to be 0.334 eV below the valence-band edge of GaAs. R. Dingle, W. Wiegmann, and C. H. Henry, Phys. Rev. Lett. **33**, 827 (1974), had found a 15% offset in earlier work.
[28]*Landolt-Börnstein, Numerical Data and Functional Relationships in Science and Technology,* New Series, Vol. 17a, *Semiconductors: Physics of Group IV and III-V Compounds,* edited by O. Madelung, M. Schulz, and H. Weiss (Springer-Verlag, Berlin, 1982). The room-temperature lattice constant of AlAs is actually 5.660 Å, but here we take it to be equal to the GaAs lattice constant of 5.653 Å.
[29]We have also calculated the band structure, but not the deep levels, in 2×34 and 18×18 superlattices. This requires diagonalization of 360×360 matrices.
[30]S. Y. Ren and J. D. Dow, Phys. Rev. B **38**, 1999 (1988).
[31]The defect-potential matrix elements are related to the difference in atomic energies of the impurity and the host atom it replaces:

$$V_l=\beta_l[w_{\text{impurity}}(l)-w_{\text{host}}(l)]+C_l\ ,$$

where we have $l=s$ or p, $\beta_s=0.8$, and $\beta_p=0.6$, and the atomic-orbital energies w can be found in Table III of Ref. 25. The constant C_l is zero in Refs. 20 and 25, but here we take $C_s=1.434$ eV in order to have the Si deep level in GaAs appear 0.234 eV above the conduction-band minimum, where it is observed (Ref. 3), instead of 0.165 eV below it, thereby compensating for the small theoretical uncertainty. In order to simplify the presentation of the results for the a_1 states, we use Hjalmarson's rule:[32] $V_s-C_s=2V_p$, thereby displaying E for the a_1 states as a function of V_s alone for the s-like state and as a function of V_p alone for the p_z-like state.
[32]H. P. Hjalmarson (private communication). This rule has been widely used in other contexts, most often with $C_l=0$: See, for example, J. D. Dow, R. E. Allen, and O. F. Sankey, in *The Chemistry and Physics of Solid Surfaces V,* Vol. 35 of *Springer Series in Chemical Physics,* edited by R. Vanselow and R. Howe (Springer-Verlag, Berlin, 1984).
[33]D. J. Chadi and M. L. Cohen, Phys. Rev. B **8**, 5747 (1973).
[34]J. N. Schulman and T. C. McGill, Phys. Rev. B **19**, 6341 (1979).
[35]A. C. Gossard, P. M. Petroff, W. Weigmann, R. Dingle, and A. Savage, Appl. Phys. Lett. **29**, 323 (1976).
[36]For a review of deep-level theories, see, for example, Ref. 21 and references therein.
[37]W. A. Harrison, *Electronic Structure and the Properties of Solids* (Freeman, San Francisco, 1980).
[38]L. A. Hemstreet, Phys. Rev. B **15**, 834 (1977); P. Vogl and J. Baranowski, Acta Phys. Polonica **A67**, 133 (1985); M. Scheffler, J. P. Vigneron, and G. B. Bachelet, Phys. Rev. Lett. **49**, 1765 (1982); J. Bernholc, N. O. Lipari, S. T. Pantelides, and M. Scheffler, Phys. Rev. B **26**, 5706 (1982); M. Jaros and S. Brand, *ibid.* **14**, 4494 (1976); U. Lindefelt, J. Phys. C **12**, L419 (1979); D. A. Papaconstantopoulos and E. N. Economou, Phys. Rev. B **22**, 2903 (1980); G. A. Baraff and M. Schlüter, Phys. Rev. Lett. **41**, 892 (1978); Phys. Rev. B **19**, 4965 (1979); J. Bernholc and S. T. Pantelides, *ibid.* **18**, 1780 (1978); J. Bernholc, N. O. Lipari, and S. T. Pantelides, Phys. Rev. Lett. **41**, 895 (1978); Phys. Rev. B **21**, 3545 (1980); J. Bernholc, S. T. Pantelides, N. O. Lipari, and A. Baldereschi,

Solid State Commun. **37**, 705 (1981).

[39]The deep-level energies are comparably independent of N_2.

[40]S. Y. Ren, J. D. Dow, and D. J. Wolford, Phys. Rev. B **25**, 7661 (1982).

[41]D. J. Wolford, J. A. Bradley, K. Fry, and J. Thompson, in *Proceedings of the 17th International Conference on the Physics of Semiconductors*, edited by D. J. Chadi and W. A. Harrison (Springer-Verlag, New York, 1984), p. 627.

[42]X. S. Zhao, G. H. Li, H. X. Han, Z. P. Wang, R. M. Tang, and R. Z. Che, Acta. Phys. Sin. **33**, 588 (1984) [Chinese Phys. **5**, 337 (1985)].

[43]M. Lannoo and P. Lenglart, J. Phys. Chem. Solids **30**, 2409 (1969).

[44]M. S. Daw and D. L. Smith, Phys. Rev. B **20**, 5150 (1979); Solid State Commun. **37**, 205 (1981); J. Vac. Sci. Technol. **17**, 1028 (1980); Appl. Phys. Lett. **36**, 690 (1980); M. S. Daw, D. L. Smith, C. A. Swarts, and T. C. McGill, J. Vac. Sci. Technol. **19**, 508 (1981).

[45]For $Al_{0.7}Ga_{0.3}Ga$ and GaAs, the T_2 cation-vacancy level is predicted to lie at 0.11 and -0.04 eV, respectively, with respect to the relevant valence-band maximum.

[46]See, for example, J. P. Buisson, R. E. Allen, and J. D. Dow, J. Phys. (Paris) **43**, 181 (1982); E. S. Ho and J. D. Dow, Phys. Rev. B **27**, 1115 (1983).

[47]The abscissae of Figs. 7 and 8 are, to within an additive constant,[31] $\beta_s w(s)$ and $\beta_p w(p)$, where the atomic-orbital energies in the solid w are tabulated in Ref. 25, and we have $\beta_s = 0.8$ and $\beta_p = 0.6$.

[48]H. P. Hjalmarson (private communication).

[49]H. P. Hjalmarson, Ph.D. thesis, University of Illinois at Urbana-Champaign, 1979 (unpublished).

[50]O. F. Sankey, H. P. Hjalmarson, J. D. Dow, D. J. Wolford, and B. G. Streetman, Phys. Rev. Lett. **45**, 1656 (1980); O. F. Sankey and J. D. Dow, Appl. Phys. Lett. **38**, 685 (1981); J. Appl. Phys. **52**, 5139 (1981); Phys. Rev. B **26**, 3243 (1982).

[51]M.-F. Li and P. Y. Yu, Solid State Commun. **61**, 13 (1987); M.-F. Li, P. Y. Yu, E. R. Weber, and W. Hansen, Appl. Phys. Lett. **51**, 349 (1987).

[52]A casual examination of the theory, Fig. 7, indicates that Sn should have a deep level $\simeq 0.4$ eV above the Si level (with B in between). However, Sn experimentally lies only 0.056 eV above Si in GaAs,[3] the difference being attributable within the current theory to lattice relaxation. Hence Sn doping rather than Si doping is unlikely to represent much of an improvement in small-period superlattices.